Simulation of ionic crystals: The *ab initio* perturbed-ion method and application to alkali hydrides and halides

Víctor Luaña*
Departamento de Matemáticas, y Departamento de Química Física y Analítica, Facultad de Química, Universidad de Oviedo, E-33007 Oviedo, Spain

L. Pueyo
Departamento de Química Física y Analítica, Facultad de Química, Universidad de Oviedo, E-33007 Oviedo, Spain
(Received 18 April 1989; revised manuscript received 28 July 1989)

A new theoretical scheme appropriate for studying the electronic structure of ionic crystals is presented and applied to nine AB-type cubic lattices (A = Li, Na, K; B = H, F, Cl). The scheme, called the *ab initio* perturbed-ion (PI) method, is based on the theory of electronic separability and the *ab initio* model-potential approach of Huzinaga. In the PI method, the self-consistent-field (SCF) equations for each different lattice ion are first solved in a lattice potential that contains nuclear attraction, Coulombic, and nonlocal exchange operators, and lattice projectors enforcing the required ion-lattice orthogonality. The ionic SCF solutions are then used to compute the lattice potential, and the process is repeated until ion-lattice consistency is achieved. The lattice energy and other equilibrium properties are immediately obtained from the PI wave functions. The most remarkable ideas suggested by this crystal simulation are the following: (a) The crystal potential produces a contraction of the free-ion valence radial density, large for the anions but very small for the cations, that works as a bonding mechanism able to describe accurately the stability and equilibrium elastic constants of simple ionic crystals; (b) the PI method explains well the variation of several crystal properties with hydrostatic pressure; (c) the crystal bonding can be clearly analyzed in terms of simple cationic and anionic contributions. Moreover, the PI code may be used as an efficient source of environment-consistent ionic wave functions and energies.

I. INTRODUCTION

The cluster approximation is a traditional approach to the study of the electronic structure of transition-metal ions in ionic crystals. It was first applied in a nonempirical manner to $KNiF_3$ by Sugano and Shulman.[1] Since then many cluster calculations on pure crystals and impurity systems like Cu^+:NaF have been reported. Some important recent works are those in Refs. 2–11. These studies have shown that although the cluster approximation gives, in general, reasonably accurate descriptions of the localized electronic states, an adequate treatment of the cluster-lattice interaction is a necessary component of the calculation.

In using the cluster approximation, one has to pay attention to the following three broad questions: (a) the description of the finite cluster, (b) the description of the extracluster lattice ions required to compute the cluster-lattice interaction, and (c) the mathematical and physical consistency between these two descriptions. A rigorous molecular-structure method is required in dealing with the first equation. Questions (b) and (c) have received less attention and are far from being completely solved at the present time. In many instances, the lattice ions have been disregarded or simulated by point charges, and question (c) neglected.[12]

Recently, some authors have considered a quantum-mechanical description of the lattice ions.[6–11] Winter, Pitzer, and Temple[6–8] have used total ion potentials for the cluster nearest neighbors. Barandiarán and Seijo[11] have remarked upon the significance of the cluster-lattice orthogonality and have taken care of it by means of the *ab initio* model-potential (MP) description[13] of the crystal. Kunz and co-workers[9,10,14] have discussed the cluster-lattice consistency and have developed lattice-consistent localizing potentials to compute the total energy of the cluster.

We have recently investigated the cluster approximation[15–18] in the light of the theory of electronic separability[19,20] (TES) and the *ab initio* MP approach of Huzinaga and co-workers.[11,12] These studies suggested the idea of analyzing a limiting case of the cluster approximation in which a cluster reduced to a single center is coupled to a crystal lattice through a rigorous quantum-mechanical cluster-lattice interaction. The outcome of this approach is a new crystal model based on the idea of ion-lattice consistency. We have called it the *ab initio* perturbed-ion (PI) method. In this paper we present the PI method and an application to simple ionic crystals. A preliminary report has been given elsewhere.[21]

In the PI method we assume that the crystal electronic density is a sum of the densities of the individual ions. We obtain the best wave function for each different lattice ion (the "cluster") by minimizing its effective energy in the field of the crystal lattice. The effective energy is written as a sum of the intraionic energy, or net energy of

the ion, and the ion-lattice interaction energy. The latter is the expectation value, in the cluster space, of an operator made of the lattice effective potential (containing nuclear attraction and Coulomb and nonlocal exchange operators) and the lattice-projection operator that enforces the cluster-lattice orthogonality. The best ionic wave functions are then used to compute the lattice effective potential and the lattice projector. The process is iterated until convergence in a way that resembles the method of the lattice-consistent localizing potentials of Kunz and Klein.[14]

The output of the PI method is a set of crystal wave functions and orbital, net, and effective energies for each different lattice ion. The lattice energy is immediately computed from the net and interaction ionic energies. The equilibrium geometry and elastic constants of the crystal are obtained from this energy. The zero-temperature Gibbs free energy of the crystal is readily written as a function of the external pressure and the lattice parameters. Crystal properties like polymorphic transition pressures are then predicted[22,23] from the Gibbs function.

The PI method can also be considered as a basis-set generator, useful as an auxiliary tool in complex cluster calculations. This use of the ionic PI orbitals would follow the suggestions of Yamashita and Kojima,[24] Hosino *et al.*,[25] and Katsuki,[26] who emphasized the necessity of using lattice-consistant ionic wave functions rather than Hartree-Fock free-ion orbitals in solid-state calculations. On the other hand, the PI basis would be more appropriate than the free-ion basis in the analysis of a large variety of experiments on ion crystals.[27,28]

We have applied here the PI method to the study of the chemical bonding, equilibrium properties, and response to the hydrostatic pressure of several alkali hydrides and halides. These systems have been extensively analyzed in the literature by different theoretical methods. Their electron-energy band structures have been recently discussed by Kunz[29] and by Yamashita and Asano.[30,31] Bonding and equilibrium properties were discussed in detail by Gordon and co-workers[22,23] in terms of nonempirical pair-potential theory. The cluster model has also been applied to the alkali halides. Menzel *et al.*[32] reported several cluster calculations on LiF directed to compare this approach with the infinite-crystal analysis. More recently, Winter, Pitzer, and Temple presented cluster calculations for pure NaF (Ref. 6) and NaCl (Ref. 7), and Winter and Pitzer[8] for pure MgF_2, in their studies of transition-metal impurities in these halides. Being a cluster calculation, the present work can be related not only to the latter cluster analyses, but also to the local-orbital procedures of Kunz.[29] The lattice-induced orbital deformation appearing in the PI method is also related to that discussed by Boyer *et al.*[33] in the potential-induced breathing model.

Our results show that the PI procedure is an accurate algorithm for the prediction of electron densities, equilibrium geometry, lattice energy, and elastic constants of simple ionic systems. The response of the NaF to the external pressure is well described by the PI method up to about 20 GPa. These results suggest that the cluster approximation can work very well if the cluster-lattice consistency is secured and the cluster-lattice interaction is accurately computed, even if the cluster is reduced to a single ion.

The present version of the PI algorithm can be improved in order to deal with open-shell systems and electron correlation. We are presently working in these questions. Further applications of the PI method to more complex fluorides and oxides are also in progress.

The layout of the paper is as follows. Section II is dedicated to the formulation of the PI method. Section III contains our results for nine halides and hydrides computed at the observed equilibrium geometry. In Sec. IV we report the PI description of the response of NaF to the hydrostatic pressure.

II. THE *AB INITIO* PI METHOD

According to the TES,[16,17,19,20,34] if a system can be partitioned into weakly interacting groups, its electronic wave function can be written as an antisymmetrized product of group wave functions. If these satisfy strong-orthogonality conditions,[35,36] the total energy of the system is the sum of intragroup or net energies and intergroup interaction energies. We are interested in the wave function Ψ_A of a particularly relevant group, the active (A) group, whose self-consistent-field (SCF) equations are solved in the field of the remaining (frozen) groups. All contributions of the A group to the total energy can be collected in the effective energy

$$E^A_{\rm eff}=E^A_{\rm net}+\sum_{R\ (\neq A)}E^{AR}_{\rm int}=E^A_{\rm net}+E^A_{\rm int} \tag{1}$$

that gives by minimization the best Ψ_A for a set of given frozen groups.

The total energy of the system is not the sum of the group effective energies. However, we can define the additive energy of the A group as

$$E^A_{\rm add}=E^A_{\rm net}+\tfrac{1}{2}\sum_{R\ (\neq A)}E^{AR}_{\rm int}=E^A_{\rm net}+\tfrac{1}{2}E^A_{\rm int} \tag{2}$$

and see that the total energy of the $A_aB_bC_c\cdots$ system is the sum

$$E=aE^A_{\rm add}+bE^B_{\rm add}+cE^C_{\rm add}+\cdots\ . \tag{3}$$

If the frozen groups can be described by single Slater determinants, $E^A_{\rm eff}$ can be derived from an effective electronic Hamiltonian:[19,20]

$$E^A_{\rm eff}({\rm elec})=\langle\Psi_A|H^A_{\rm eff}|\Psi_A\rangle \tag{4}$$

with

$$H^A_{\rm eff}=\sum_{i=1}^{N_A}h^A_{\rm eff}(i)+\sum_{1\le j<i\le N_A}r_{ij}^{-1}\ , \tag{5}$$

$$h^A_{\rm eff}(i)=\left[T(i)-\sum_{\alpha=1}^{\nu_A}Z^A_\alpha r_{iA}^{-1}\right]+\sum_{S\ (\neq A)}[V^S_{\rm eff}(i)+P^S(i)]\ , \tag{6}$$

where i,j run over the N_A electrons of the active group, α and β over its ν_A nuclei, and S over frozen groups. $V^S_{\rm eff}(i)$ represents the potential energy of the ith electron of the active group in the field of the S frozen group:

$$V^S_{\rm eff}(i)=-\sum_{\sigma=1}^{\nu_S} Z^S_\sigma r^{-1}_{iS}+V^S_C(i)+V^S_X(i)\ . \tag{7}$$

The projector $P^S(i)$ in Eq. (6) represents the orthogonality constraints between the active group and the S frozen group. For closed-shell ions, this operator can be written in the form[13,37,38]

$$P^S(i)=\sum_{g\in S}|\psi^S_g\rangle(-2\varepsilon^S_g)\langle\psi^S_g|\ , \tag{8}$$

where g runs over all occupied orbitals ψ_g with orbital energies ε^S_g.

The effective energy is the energy in Eq. (4) plus the nuclear term

$$E^A_{\rm eff}({\rm nuc})=-\sum_{\alpha=1}^{\nu_A}\sum_{S\ (\neq A)} Z^A_\alpha V^S_{\rm eff}(\mathbf{R}_\alpha) + \sum_{1\le\beta<\alpha\le\nu_A} Z^A_\alpha Z^A_\beta R^{-1}_{\alpha\beta}\ , \tag{9}$$

where $V_{\rm eff}(\mathbf{R}_\alpha)$ is the effective potential of the S group at the α nucleus of the active group. Only the nuclear-attraction and Coulombic-repulsion terms of the effective potential contribute to this nuclear effective energy.

These are the basic equations of the TES. To complete a calculation within this framework one has to select (a) a meaningful partition of the system into active and frozen groups, (b) an adequate basis set to describe the frozen groups, and (c) an approximate form for the effective potential.

The *ab initio* PI method is a TES-consistent algorithm defined by a particular answer to these three requirements, as follows. We consider each different lattice ion as the active group. The lattice effective potential and projection operators are computed, as described in detail to follow, in terms of a trial basis set. The SCF equations are solved for all different ions at each PI cycle and their solutions transferred to the lattice. The PI cycles are repeated until ion-lattice consistency is reached. For a given set of primitive functions, the PI calculation gives the coefficients that minimize the effective energy of all different lattice ions.

Let us see now the form of the effective potential. For the closed-shell system considered in this paper, the Coulombic part is given by

$$V^S_C(r_1)=\int\rho^S(r_2)r^{-1}_{12}\,d\tau_2\ , \tag{10}$$

where $\rho^S(r)$ is the radial density of the S ion. This form can be accurately represented by the Bonifacic-Huzinaga equation.[39]

The exchange part can be written as the nondiagonal spectral resolution:[11,13]

$$V^S_X(i)=-\sum_{l}\sum_{m=-l}^{l}\sum_{a,b}|alm,S\rangle A(l,ab,S)\langle blm,S|\ , \tag{11}$$

where $\{|alm,S\rangle\}$ are products of spherical harmonics and primitive radial functions for the S ion. $A(l,ab,S)$ are the elements of the matrix

$$\mathbf{A}=\mathbf{S}^{-1}\mathbf{K}\mathbf{S}^{-1} \tag{12}$$

and $\mathbf{S}$ and $\mathbf{K}$ the overlap and exchange matrices for the S ion in $\{|alm,S\rangle\}$.

This effective potential has the following asymptotic limits:

$$\lim_{r\to0} rV^S_{\rm eff}(r)=-Z^S\ , \tag{13}$$

$$\lim_{r\to\infty} rV^S_{\rm eff}(r)=-(Z^S-N_S)=-z^S\ , \tag{14}$$

where N_S is the number of electrons of the S ion.

This formulation of the TES can be easily adapted to any atomic or molecular SCF program. We have used a Roothaan-Bagus program[40] to write the PI code.[41] This is a highly efficient code that performs four independent calculations: (a) basic one-center integrals S, T, U, P, and Q (Ref. 40), (b) matrix elements of the effective potential and lattice operators, (c) an atomic SCF process with or without ion-lattice interaction, and (d) generation of the effective potentials. The PI atomic orbitals (AO's) have identical radial functions for all subspecies of a given symmetry. This treatment is exact for sp ions located at octahedral or cubic sites.

III. THE *AB INITIO* PI DESCRIPTION OF THE ALKALI HYDRIDES AND HALIDES

A. The crystal model

At room temperature and pressure, the nine crystals analyzed here show the rocksalt structure (see Table I). We will consider a collection of ionic layers surrounding the active ion, the ith layer containing N_i equivalent ions at the same distance R_i from the active ion. In Table II we list the characteristics of the first 15 layers. Only the closer layers will contribute to the lattice-projection energy of the active ion because the overlap integrals appearing in the expectation values of the lattice projectors are exponentially decreasing functions of the interionic distance. The effective potentials tend to reach the pointlike asymptotic limit at rather short distances. We have integrated the projection operators and effective potentials for the first ten layers. This represents 170 ions with $a/2\le R_i\le 11^{1/2}a/2$. From Table I we see that $11^{1/2}a/2$ is 6.68 Å for LiF and 10.44 Å for KCl. Lattice ions at larger distances give vanishing projection energy and

TABLE I. Experimental cell constants, a (in Å), for alkali hydrides and halides AB (with A=Li,Na,K, and B=H,F,Cl).

	H[a]	F[b]	Cl[b]
Li	4.08	4.028	5.140
Na	4.88	4.634	5.640
K	5.70	5.348	6.294

[a]Reference 60.
[b]Reference 56.

TABLE II. Characteristics of the ionic layers surrounding a cation in the rocksalt structure. (Note that the positions of all ions in a layer are given by all combinations of the indicated coordinates and signs.)

Layer number	Type of ion	Number of ions	Ionic coordinates[a]	R_l [a]
1	Cl	6	(±1,0,0)	1
2	Na	12	(±1,±1,0)	$2^{1/2}$
3	Cl	8	(±1,±1,±1)	$3^{1/2}$
4	Na	6	(±2,0,0)	$4^{1/2}$
5	Cl	24	(±2,±1,0)	$5^{1/2}$
6	Na	24	(±2,±1,±1)	$6^{1/2}$
7	Na	12	(±2,±2,0)	$8^{1/2}$
8	Cl	24	(±2,±2,±1)	$9^{1/2}$
8	Cl	6	(±3,0,0)	$9^{1/2}$
9	Na	24	(±3,±1,0)	$(10)^{1/2}$
10	Cl	24	(±3,±1,±1)	$(11)^{1/2}$
11	Na	8	(±2,±2,±2)	$(12)^{1/2}$
12	Cl	24	(±3,±1,±0)	$(13)^{1/2}$
13	Na	48	(±3,±2,±1)	$(14)^{1/2}$
14	Na	6	(±4,0,0)	$(16)^{1/2}$
15	Cl	24	(±4,±1,0)	$(17)^{1/2}$
15	Cl	24	(±3,±2,±2)	$(17)^{1/2}$

[a]In units of $a/2$.

contribute to the effective energy of the active ion through the term

$$V_{\text{ext}}(\mathbf{r}) = -\sum_S z^S/|\mathbf{r}-\mathbf{R}_S| \ . \tag{15}$$

As described in detail in Ref. 17, we compute $V_{\text{ext}}(\mathbf{r})$ by the Ewald method,[42–45] and approximate it by the accurate one-electron operator:

$$V_{\text{fit}}(\mathbf{r}) = C_1 + \sum_{k=2}^{6} C_k r^k + C_7 r^8 + (C_8 r + C_9 r^2 + C_{10} r^3)(x^2y^2 + y^2z^2 + z^2x^2)$$
$$+ (C_{11} + C_{12} r)(x^6 + y^6 + z^6) + C_{13}(x^8 + y^8 + z^8) + (C_{14} r + C_{15} r^2)(x^2y^2z^2) \ , \tag{16}$$

where the C_i's are fitting parameters. This form reproduces the Ewald values within 3×10^{-5} hartree at any point inside a sphere of radius 7 Å centered at the nucleus of the A ion.

We have used the optimized 4s Slater-type orbital (STO) basis of Table III for the H^- ion, and the STO bases of Clementi and Roetti[46] for the remaining ions: 4s (Li^+), 5s4p (Na^+), 5s5p (F^-), 7s5p (K^+), and 7s6p (Cl^-). These bases are very close to the Hartree-Fock (HF) limit. The coefficients of these atomic orbitals have been used as trial vectors.

TABLE III. Optimized (4s) STO basis set for the $1s^2\,{}^1S$ ground state of the H^- ion. All entries in atomic units.

Basis	1s
Orbital energy:	−0.046 22
1s 1.513 429	0.149 999 2
1s 0.779 085	0.427 703 3
1s 0.404 876	0.454 056 1
1s 0.284 763	0.045 344 3
HF total energy:	−0.487 930
Potential energy:	−0.975 857
Kinetic energy:	0.487 927
Virial ratio:	−2.000 005
$\langle r\rangle_{1s}$ = 2.503 393 6	

B. Convergence of the PI calculation

As described before, the PI algorithm proceeds by a series of cycles starting from a trial basis set. In the crystals studied here convergence is reached after a short number of cycles (see Fig. 1). These energies converge within 10^{-4} hartree in 3–4 cycles and significant changes in the basis sets appear just in the first cycle. This pattern is followed in all other cases, although the convergence process tend to be somewhat slower for crystals involving smaller ions. Properties other than orbital energies converge in a parallel manner.

C. Lattice effects on the electronic energy levels

In Table IV we present PI valence orbital energies and interaction energies for the nine crystals considered here. It is interesting to compare the interaction energy, which

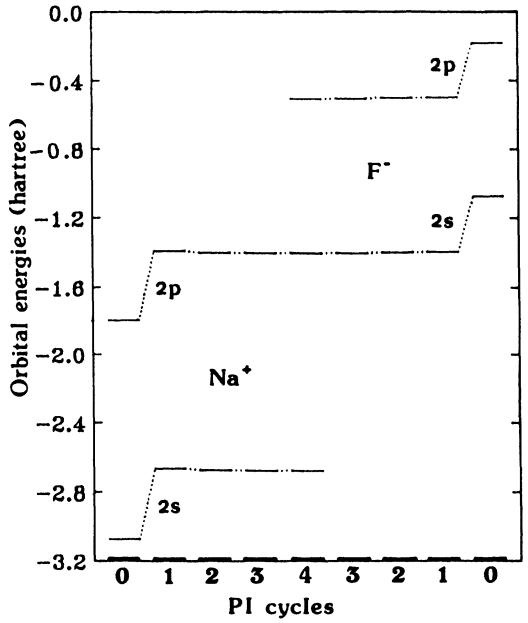

FIG. 1. Orbital energies of the Na^+ and F^- ions for the first four cycles of the PI calculation on NaF.

is a rough measure of the energy involved in the process of crystal formation, with the orbital energies. In Table IV we see that the interaction energy ranges from -0.23 to -0.45 hartree. Also, we observe that there are not cationic orbital energies within these limits and that all states of the halide anions are well below this range, with the exception of the highest occupied *np* state. The 1*s* energy of the hydride ion lies also within this range.

All cationic AO's and those anionic AO's having orbital energies outside the range spanned by the interaction energy are essentially unaffected by the process of crystal formation. Only the 1*s* orbital of the hydride ion and the *np* highest occupied orbital of the halide ions suffer noticeable deformation upon lattice formation. These results suggest that an orbital would be affected by a lattice potential if its energy is close to the ion-lattice interaction energy. Since the Madelung energy is a good approximation to the interaction energy, this conjecture could be a useful rule in the search for ionic systems with appreciable lattice-induced orbital deformations.

The cationic orbital energies increase and the anionic energies decrease along the PI process. To simplify the discussion we use the average shift

$$\langle \Delta\varepsilon \rangle = \sum_i N_i(\varepsilon_i^{\mathrm{PI}} - \varepsilon_i^{\mathrm{free}}) \Big/ \sum_i N_i \ , \tag{17}$$

where i runs over the occupied levels of the ion, N_i is the number of electrons in the ith level, and $\varepsilon_i^{\mathrm{PI}}$ and $\varepsilon_i^{\mathrm{free}}$ are orbital energies of the ith level in the PI and free-ion descriptions, respectively. It is also useful to observe the typical deviation of the energy shifts from the average in Eq. (17). These numbers are collected in Table V.

TABLE IV. PI valence orbital energies and interaction energies (in hartrees). [Note that the numbers appearing below each orbital energy are the differences ε(PI) − ε(free ion).]

Crystal	Cation		Anion		Crystal	Cation		Anion	
LiH	(1*s*):	−2.355 63	(1*s*):	−0.315 95	LiCl	(1*s*):	−2.432 71	(3*s*):	−0.996 15
		0.436 75		−0.269 73			0.359 67		−0.263 20
	E_{int}:	−0.430 14	E_{int}:	−0.355 77				(3*p*):	−0.409 28
									−0.259 36
						E_{int}:	−0.356 67	E_{int}:	−0.309 80
NaH	(2*s*):	−2.699 16	(1*s*):	−0.282 32	NaCl	(2*s*):	−2.746 32	(3*s*):	−0.979 87
		0.374 49		−0.236 10			0.327 33		−0.246 92
	(2*p*):	−1.423 53				(2*p*):	−1.468 75	(3*p*):	−0.395 79
		0.373 62					0.328 40		−0.245 87
	E_{int}:	−0.377 87	E_{int}:	−0.325 72		E_{int}:	−0.329 56	E_{int}:	−0.289 60
KH	(3*s*):	−1.645 54	(1*s*):	−0.237 03	KCl	(3*s*):	−1.672 22	(3*s*):	−0.947 09
		0.318 90		−0.190 81			0.292 22		−0.214 14
	(3*p*):	−0.852 01				(3*p*):	−0.875 40	(3*p*):	−0.365 42
		0.319 08					0.295 69		−0.215 50
	E_{int}:	−0.325 45	E_{int}:	−0.280 68		E_{int}:	−0.291 53	E_{int}:	−0.230 39
LiF	(1*s*):	−2.335 18	(2*s*):	−1.447 12	NaF	(2*s*):	−2.676 77	(2*s*):	−1.403 16
		0.457 20		−0.372 68			0.396 88		−0.328 72
			(2*p*):	−0.548 74		(2*p*):	−1.400 54	(2*p*):	−0.506 28
				−0.367 89			0.396 61		−0.325 43
	E_{int}:	−0.445 56	E_{int}:	−0.430 26		E_{int}:	−0.386 06	E_{int}:	−0.386 65
KF	(3*s*):	−1.618 71	(2*s*):	−1.338 38					
		0.345 73		−0.263 94					
	(3*p*):	−0.821 25	(2*p*):	−0.447 23					
		0.349 84		−0.266 38					
	E_{int}:	−0.325 41	E_{int}:	−0.301 27					

TABLE V. Average shifts, Eq. (17), and relative deviations shown by the ionic orbital energies upon crystal formation (in hartrees).

Crystal	Madelung energy	Cation ⟨Δε⟩	Cation Deviation	Anion ⟨Δε⟩	Anion Deviation
LiH	+0.453 32	+0.436 75		−0.269 73	
NaH	+0.379 00	+0.373 85	0.000 36	−0.236 10	
KH	+0.324 48	+0.319 16	0.000 12	−0.190 81	
LiF	+0.459 17	+0.457 20		−0.356 06	0.027 53
NaF	+0.399 12	+0.397 35	0.001 42	−0.315 27	0.023 19
KF	+0.345 84	+0.351 94	0.003 19	−0.256 19	0.020 22
LiCl	+0.359 83	+0.359 67		−0.227 62	0.030 26
NaCl	+0.327 93	+0.328 47	0.000 84	−0.218 34	0.025 69
KCl	+0.293 86	+0.296 88	0.002 18	−0.188 57	0.024 60

We see that the cationic energy shifts are very close to the Madelung potential at the cationic site. Shifts for different cationic orbitals are very similar, as revealed by the small typical deviations. It appears that the response of the cations to the PI algorithm is mainly determined by the electrostatic ion-lattice interaction. On the other hand, the stabilization shown by the energy levels of the anions is about 50–70 % of the Madelung potential at the anionic site. Deviations from the average shift are larger than those obtained for the cations. Thus, the response of the anions deviates significantly from point-charge electrostatics, as it should for these more deformable and polarizable entities.

D. Lattice effects of ionic wave functions and charge densities

In Fig. 2 we plot the PI cationic and anionic radial densities for LiH, NaF, and KCl. The other six crystals show analogous behavior. The PI cationic densities practically coincide with the free-ion values. However, we observe a contraction of the hydride density and analogous although smaller effects for the fluoride and the chloride ions. The deformations of the halides appear in the outer region of the density, the core regions remaining nearly unchanged. All these results agree with those reported by Kunz.[29]

Plots in Fig. 2 are poor indicators of the response of the valence orbitals to the lattice potential because the almost unaffected inner orbitals dominate the charge density. For this reason it is convenient to examine separately the highest occupied anionic orbitals, as we do in Fig. 3. A clear contraction of these orbitals as apparent, the effect being larger for lithium crystals. The behavior of these orbitals in the sodium and potassium salts is very similar, in spite of the rather different cell constant. This suggests that the size and electronic properties of these anions in the crystals considered here should be nearly the same.

The orbital deformation revealed by the PI calculation is quite important in the outer tail of the external anionic orbitals, but it is almost nil in the inner parts. Thus, inner operators such as the spin-orbit coupling would give very similar expectation values within the Hartree-Fock and PI bases. However, more external properties like the two-center overlaps will be rather different in these two bases.

E. Bonding and cohesive energy

We will see now how the PI method describes the crystal binding without resorting to the familiar molecular-like delocalized orbitals. Numbers in Table VI reveal that the interaction energy is, in general, a small part of

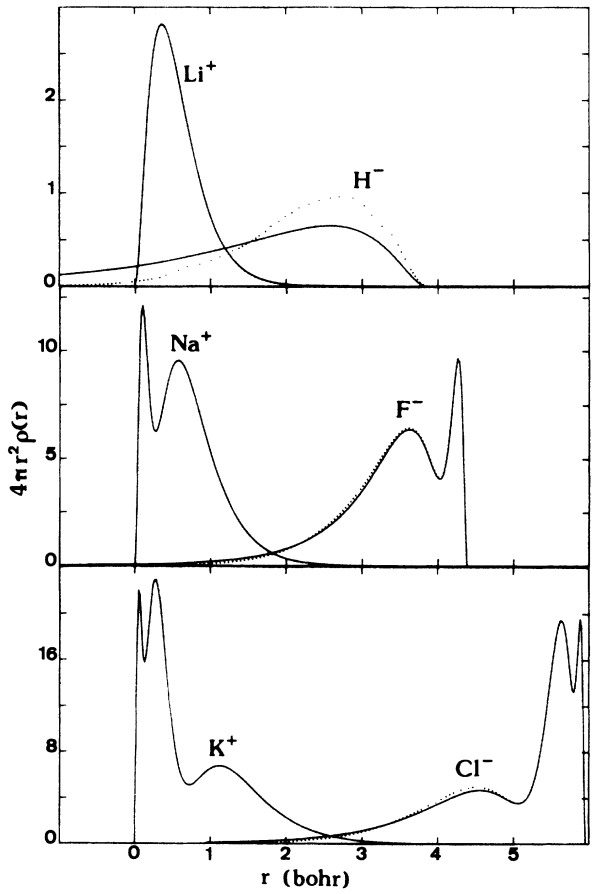

FIG. 2. Free-ion (solid lines) and PI (dotted lines) radial densities for LiH, NaF, and KCl.

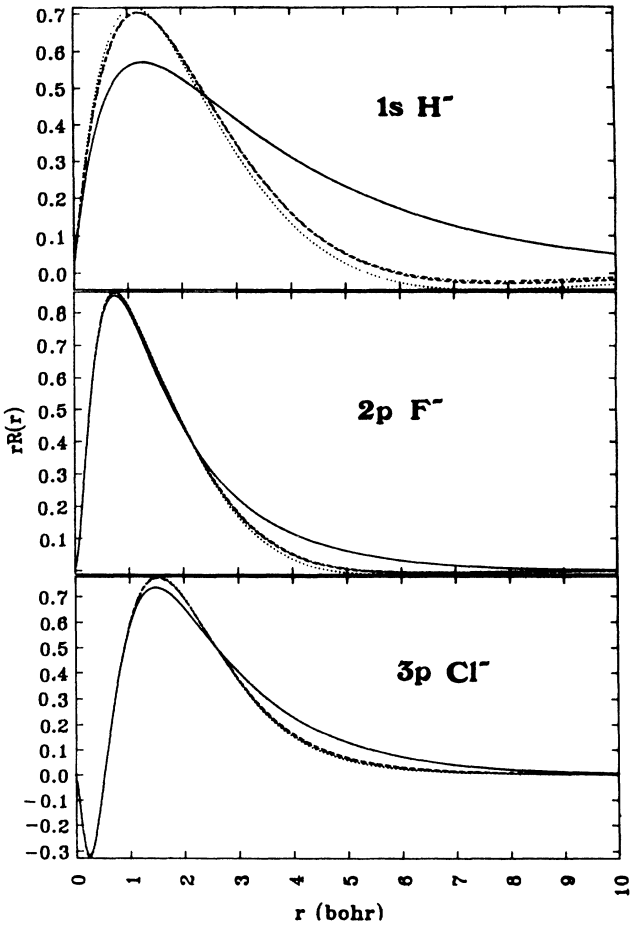

FIG. 3. Radial wave functions of the outermost valence orbital of the H^-, F^-, and Cl^- ions. Free-ion functions are plotted in solid lines; dotted, dashed, and dotted-dashed lines are used for the PI solutions in lithium, sodium, and potassium crystals, respectively.

the effective energy, the hydride ion being a noticeable exception. Cations and anions are stabilized by the ion-lattice interaction energy. The crystal energy per molecule is obtained though Eq. (3):

$$E_{\text{cryst}}=E^C_{\text{add}}+E^A_{\text{add}}=E^C_{\text{net}}+E^A_{\text{net}}+\tfrac{1}{2}(E^C_{\text{int}}+E^A_{\text{int}})\ , \tag{18}$$

where C and A stand for cation and anion, respectively. The crystal potential energy per molecule is obtained in the same way, whereas the kinetic energy is the sum of the cationic and anionic kinetic energies. The virial ratios obtained from our PI calculations (see Table VI) are greater than the exact value -2 in all these cases. According to the Hellmann-Feynman theorem, this means that in the PI description obtained at the experimental geometry there is a force tending to separate the nuclei. Thus, the internuclear distances predicted by the PI method will be somewhat larger than the experimental ones, a trend usually found in molecular Hartree-Fock results.

The lattice energy E_{latt} in the PI method is given by

$$E_{\text{latt}}=E_{\text{cryst}}-E^C_0-E^A_0\ , \tag{19}$$

where the subscript 0 stands for free-ion values. E_{latt} can be written in an interesting form by introducing Eq. (18) into Eq. (19):

$$\begin{aligned}E_{\text{latt}}&=(E^C_{\text{net}}-E^C_0)+(E^A_{\text{net}}-E^A_0)+\tfrac{1}{2}E^C_{\text{int}}+\tfrac{1}{2}E^A_{\text{int}}\\&=E^C_{\text{def}}+E^A_{\text{def}}+\tfrac{1}{2}E^C_{\text{int}}+\tfrac{1}{2}E^A_{\text{int}}\\&=E^C_{\text{bind}}+E^A_{\text{bind}}\ ,\end{aligned} \tag{20}$$

where we have defined the deformation energy of the K ion as

$$E^{\text{K}}_{\text{def}}=E^{\text{K}}_{\text{net}}-E^{\text{K}}_0 \tag{21}$$

and the binding energy of the K ion as

$$E^{\text{K}}_{\text{bind}}=E^{\text{K}}_{\text{def}}+\tfrac{1}{2}E^{\text{K}}_{\text{int}}\ . \tag{22}$$

According to Eq. (20), we can partition the lattice energy into a sum of cationic and anionic binding contributions each made, in turn, of two factors [Eq. (22)]: one that measures the energy associable to the orbital deformation, E_{def}, and another one that is one-half of the interaction energy of the ion. The first factor cannot be

TABLE VI. Energy terms related to the lattice formation (in hartrees).

(a) Total energy of the free ions

H^-	F^-	Cl^-	Li^+	Na^+	K^+
−0.487 93	−99.459 37	−459.576 70	−7.236 41	−161.676 92	−599.017 30

(b) Ionic energies in the crystals

	Anion		Cation		Crystal	
	E_{eff}	E_{net}	E_{eff}	E_{net}	E_{cryst}	Virial
LiH	−0.749 81	−0.394 04	−7.666 38	−7.236 26	−8.023 24	−1.988 57
NaH	−0.740 01	−0.414 29	−162.054 79	−161.676 92	−162.443 00	−1.999 92
KH	−0.696 44	−0.415 77	−599.342 76	−599.017 30	−599.736 14	−1.999 95
LiF	−99.836 40	−99.406 14	−7.681 20	−7.235 64	−107.079 69	−1.998 94
NaF	−99.807 59	−99.420 93	−162.062 86	−161.676 80	−261.484 09	−1.999 83
KF	−99.726 73	−99.425 46	−599.342 54	−599.017 14	−698.755 94	−1.999 78
LiCl	−459.819 45	−459.509 67	−7.592 85	−7.236 19	−467.079 08	−1.999 25
NaCl	−459.817 56	−459.527 96	−162.006 45	−161.676 89	−621.514 43	−1.999 63
KCl	−459.762 83	−459.532 44	−599.308 79	−599.017 25	−1058.810 66	−1.999 69

TABLE VII. Cationic and anionic deformation, interaction, and binding energies for several ionic crystals (in hartrees).

Crystal	E^C_{def}	$\frac{1}{2}E^C_{int}$	E^C_{bind}	E^A_{def}	$\frac{1}{2}E^A_{int}$	E^A_{bind}
LiH	0.000 15	−0.215 06	−0.214 91	0.093 89	−0.177 89	−0.084 00
NaH	0.000 00	−0.188 94	−0.188 94	0.073 64	−0.162 86	−0.089 22
KH	0.000 00	−0.162 73	−0.162 73	0.072 16	−0.140 34	−0.068 18
LiF	0.000 77	−0.222 78	−0.222 01	0.053 23	−0.215 13	−0.161 90
NaF	0.000 12	−0.193 03	−0.192 91	0.038 44	−0.193 33	−0.154 89
KF	0.000 16	−0.162 71	−0.162 55	0.033 91	−0.150 64	−0.116 73
LiCl	0.000 22	−0.178 34	−0.178 12	0.067 03	−0.154 89	−0.087 86
NaCl	0.000 03	−0.164 78	−0.164 75	0.048 74	−0.144 80	−0.096 06
KCl	0.000 05	−0.145 77	−0.145 72	0.044 26	−0.115 20	−0.070 94

negative. To see this, we recall that E_{net} and E_0 are the expectation values of the free-ion Hamiltonian in the PI and free-ion bases, respectively. Since the latter basis does minimize this expectation value, $E_{net} > E_0$. Thus, the deformation energy is always a destabilizing contribution to the ionic binding energy. The second factor is negative. Deformation and binding energies for the nine crystals studied here are collected in Table VII.

The numbers in Table VII tell us that whereas the rather passive response on the part of the cations to the PI orbital deformation leads to negligible deformation energies, the larger anionic deformation gives appreciable deformation energies (up to 50 kcal/mol). In all cases, the anionic interaction energies are larger in absolute value than the corresponding deformation energies, and so the anionic binding energies are always negative.

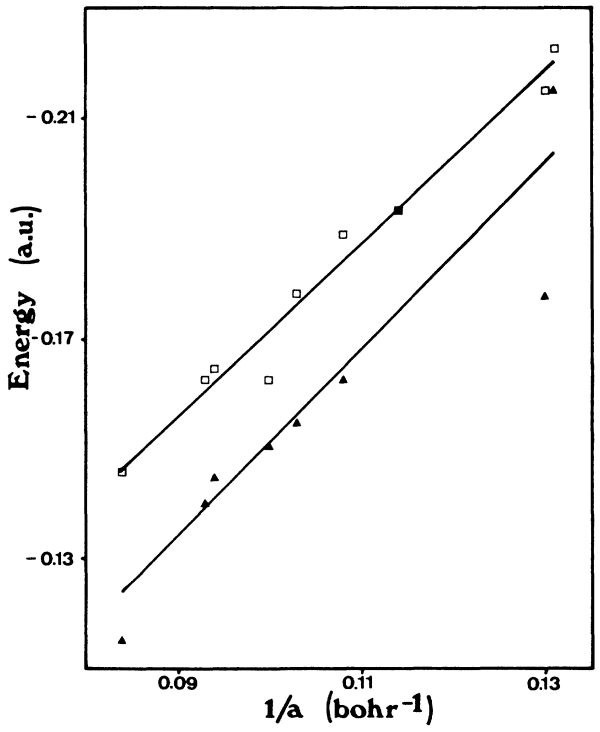

FIG. 4. PI values for cationic and anionic interaction energy vs the inverse of the observed cell constant. Open squares are used for cations and solid triangles for anions.

Since the cationic and anionic interaction energies are of the same order of magnitude, the differences in deformation energy lead to anionic binding energies smaller than their cationic counterparts. See, for instance, the LiH. Thus, the anions are much more sensitive than the cations to the orbital deformation induced by the crystal potential, but the cations give a larger contribution to the lattice energy.

Since the interaction energy plays such a significant role in determining the lattice energy, it is interesting to examine its variations from crystal to crystal. These changes are quite substantial for cations and anions, as can be seen in Table VII. In Fig. 4 we show the variation of E_{int} with the cell constant. The cationic interaction energy of these nine crystals is nearly linear in a^{-1}, in agreement with the close relationship between this quantity and the Madelung potential at the cationic site (see Tables IV and V). Anionic interaction energies show noticeable deviations from this linear relation.

Let us now see the lattice energies predicted by the PI method at the experimental geometry (Table VIII). The agreement between the PI results and the thermochemical data is remarkable for the three fluorides; it is better than that obtained by Kim and Gordon[22] and comparable to the results by Cohen and Gordon.[23,47] In the chlorides the differences are as large as 30–35 kcal/mol, rather larger than those in Ref. 22. This suggests that the PI method may describe the fluorides better than the chlorides because the former are more ionic compounds. Further research will reveal the possible correlation between the covalency and the performance of the PI method. The deviations for the hydrides (about 20–30 kcal/mol) are comparable to those obtained in Ref. 2 with a minimal basis.

Our theoretical values are generally smaller, in absolute value, than the experimental ones. Three factors can contribute to this deficiency. First, we have not optimized the equilibrium geometry of the crystal. This limitation introduces a very slight error because, as we discuss later on, the variation of the lattice energy with the cation-anion distance is very flat in the equilibrium region. Second, there is the intrinsic variational restriction in the PI method associated to the lack of mixing of cationic and anionic wave functions. This mixing would further reduce the crystal energy and thus the lattice energy. Third, we have neglected the electron correlation.

TABLE VIII. Lattice energies (in kcal/mol).

Crystal	Expt.	This work	Theor.
LiH	−217[a]	−187.6	−178,[d] −212[d]
NaH	−194[b]	−174.5	
KH	−171[b]	−144.9	
LiF	−242.3 (−246.8)[c]	−240.9	−260.2,[e] −240.5[f]
NaF	−214.4 (−217.9)[c]	−218.4	−222.3,[e] −211.9[f]
KF	−189.8 (−194.5)[c]	−175.2	−204.1,[e] −194.4[f]
LiCl	−198.9 (−201.8)[c]	−166.9	−206.1,[e] −202.0[f]
NaCl	−182.6 (−185.3)[c]	−163.7	−182.7,[e] −179.9,[f] −152[g]
KCl	−165.8 (−169.5)[c]	−136.0	−175.3,[e] −170.1[f]

[a]Reference 61.
[b]Thermochemical data from Ref. 62.
[c]Reference 43. Values in parentheses are extrapolations for $T=0$ K given by Brewer, as quoted in Ref. 55.
[d]HF calculations in Ref. 2. The first number corresponds to a minimal basis set and the second one to an extended basis.
[e]Reference 22.
[f]Reference 23.
[g]Reference 63.

We believe that the latter limitation is the more serious source of error here. The HF approximation predicts ionization potentials for the alkali-metal atoms discussed in this paper deviating 0.05–0.34 eV from the observed values (see Table IX). However, the electron affinities are seriously underestimated in this approximation. For the H^- ion, for instance, the HF value has even the wrong sign. It is sometimes argued that the HF approximation should give good lattice energies for ionic crystals because the correlation errors of the free-ion and crystal wave functions tend to cancel out. The orbital deformation induced upon crystal formation casts a serious doubt over the plausibility of this assumption.

In line with previous arguments, the correlation error could be partitioned in the PI method into cationic and anionic contributions, these contributions being the difference between the crystal and free-ion correlation errors. Since the PI and free-ion cationic densities are al-

TABLE IX. Electron affinities and ionization potentials (in eV).

(a) Electron affinities

Atom	Observed[a]	HFR[b]	ΔE_{corr}
H	0.747	−0.328	1.075
F	3.448	1.363	2.085
Cl	3.613	2.581	1.032

(b) Ionization potentials

Atom	Observed[c]	HFR[b]	ΔE_{corr}
Li	5.392	5.342	0.050
Na	5.139	4.952	0.187
K	4.341	4.006	0.335
H	13.598	13.606	
F	17.422	15.718	1.704
Cl	12.967	11.795	1.172

[a]Gas data at 0 K, Ref. 56, p. E–67.
[b]Obtained as differences of Hartree-Fock-Roothan (HFR) total energies of the atomic and ionic ground states with basis sets optimized for each state.
[c]Reference 64.

TABLE X. Theoretical diamagnetic susceptibilities for the ions and crystals studied in this work, in units of 10^{-6} $cm^3 mol^{-1}$.

(I) Susceptibility of the anion A

		A in crystals		
A	A *in vacuo*	LiA	NaA	KA
H^-	−14.905	−5.708	−5.661	−5.657
F^-	−12.640	−10.463	−10.638	−10.753
Cl^-	−30.340	−25.260	−25.885	−26.022

(II) Susceptibility of the cation C

		C in crystals		
C	C *in vacuo*	CH	CF	CCl
Li^+	−0.705	−0.698	−0.688	−0.696
Na^+	−5.079	−5.079	−5.094	−5.070
K^+	−15.496	−15.494	−15.429	−15.458

(III) Susceptibility of crystals

Crystal	HFR[a]	PI[b]	Expt.[c]
LiH	−15.610	−6.406	−4.6
NaH	−19.984	−10.740	
KH	−30.401	−21.160	
LiF	−13.345	−11.151	−10.1
NaF	−17.719	−15.745	−16.4
KF	−28.136	−26.182	−23.6
LiCl	−31.045	−25.956	−24.3
NaCl	−35.419	−30.955	−30.3
KCl	−45.836	−41.498	−39.0

[a]Sum of the free-ion values.
[b]Sum of the ionic PI values.
[c]Reference 56, p. E–124.

TABLE XI. Dimensionless Lamb term, Eq. (24).

(a) Free-ion values

	H^-	F^-	Cl^-	Li^+	Na^+	K^+
σ_L (10^{-5})	2.43	48.02	114.93	9.54	62.38	132.54

(b) PI values (10^{-5})

Crystal	Anion	Cation
LiH	3.26	9.56
NaH	3.11	62.38
KH	3.07	132.54
LiF	48.30	9.57
NaF	48.25	62.36
KF	48.24	132.57
LiCl	115.05	9.57
NaCl	115.08	62.39
KCl	115.08	132.55

most identical, the corresponding correlation errors should be nearly the same. This would give a vanishing cationic correlation-energy contribution to the lattice energy. On the contrary, the radial contraction predicted by the PI method for the anions suggests that the anionic correlation error should be larger in the crystal. In consequence, inclusion of correlation effects in the PI method should give lattice energies more negative than those presented in the present calculation.

F. Some other properties of the ionic crystals

Many useful models for different properties of ionic crystals are formulated in terms of the AO's of the constituent ions. In practice, the free-ion representation is generally adopted. It may be interesting to see the differences introduced in those analyses were the PI orbitals used instead. As a first example, we present in Table X cationic, anionic, and crystal values for the diamagnetic susceptibility:[48]

$$\chi=-(N_A e^2/6mc^2)\sum_i \langle i|r^2|i\rangle \ , \tag{23}$$

where the sum runs over all occupied spin orbitals of the ion. Cationic susceptibilities obtained with the PI wave functions differ very slightly from the free-ion values, but important deviations are found for the anions. Notice the large effect in the hydride ion. The sum of cationic and anionic PI values agrees quite well with observed crystal data, supporting the idea of ionic additivity for this quantity.

Another property that can be sensitive to the orbital deformation is the dimensionless Lamb term appearing in the electronic shielding considered in nuclear-magnetic-resonance spectroscopy. It is given by[49]

$$\sigma_L=(e^2/3mc^2)\sum_i \langle i|r^{-1}|i\rangle \ , \tag{24}$$

where the sum runs over all occupied spin orbitals of the ion. The PI values for this correction (see Table XI) are almost constant for a given ion. As expected, the differences from the free-ion values are larger for the anions, but much smaller than those obtained for the diamagnetic susceptibilities, due to the more internal character of the r^{-1} operator.

Finally, we can see the effects of the orbital deformation on the k dependence of the atomic form factors:[50]

$$F(k)=\sum_{nl} N_{nl}\int_0^\infty r^2 R_{nl}^2(r)[\sin(4\pi kr)/4\pi kr]dr \ , \tag{25}$$

where N_{nl} and $R_{nl}(r)$ are the electron occupation and the radial wave function of the nl shell of the lattice ion, respectively. The spherical form factor becomes the number of electrons in the ion when $k=0$. In Fig. 5 we have plotted the form factors for the free-ion and PI basis sets. There are significant differences only for the hydride ion. Also, our $F(k)$'s coincide with data collected in the literature.[50] The hydride form factors for LiH, NaH, and KH are very similar. They are larger than the free-ion value, at least for $0\le k\le 0.4$. From Fig. 5 we see that for a pair of isoelectronic ions, the more contracted the electron density, the larger the form factor.

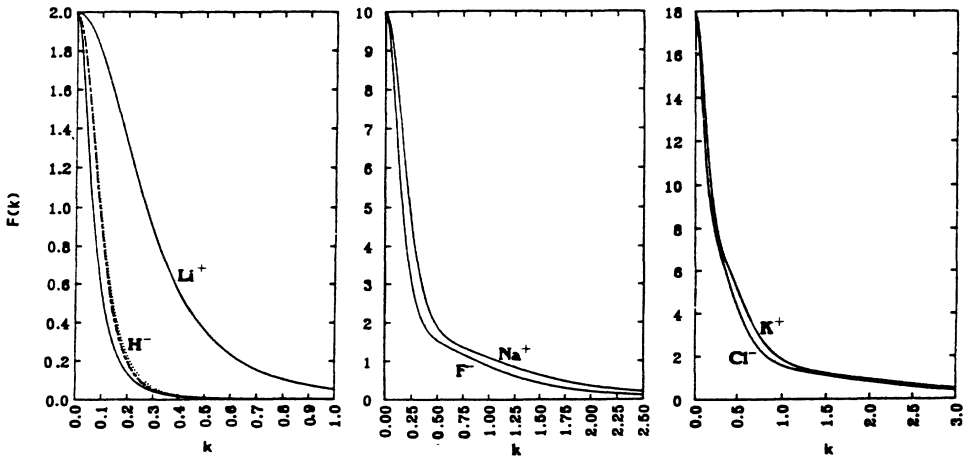

FIG. 5. Free-ion (solid lines) and crystal (dashed and dotted lines) electronic form factors.

TABLE XII. Energy terms for NaF (in hartrees) at several Na^+-F^- distances (in bohrs).

$R(Na^+$-$F^+)$	3.7	4.0	4.2	4.397	4.4	4.6	4.8	5.0
Na^+ ion								
E^C_{def}	0.001 78	0.000 59	0.000 25	0.000 12	0.000 11	0.000 05	0.000 02	0.000 01
$\frac{1}{2}E^C_{int}$	−0.212 27	−0.204 35	−0.198 56	−0.193 03	−0.192 38	−0.186 11	−0.179 92	−0.173 92
E^C_{bind}	−0.210 49	−0.203 76	−0.198 31	−0.192 91	−0.192 27	−0.186 07	−0.179 90	−0.173 91
F^- ion								
E^A_{def}	0.103 48	0.065 61	0.049 35	0.038 44	0.037 31	0.028 04	0.020 79	0.015 12
$\frac{1}{2}E^A_{int}$	−0.163 28	−0.187 50	−0.192 91	−0.193 33	−0.193 13	−0.189 61	−0.184 04	−0.177 50
E^A_{bind}	−0.059 80	−0.121 89	−0.143 56	−0.154 89	−0.155 82	−0.161 57	−0.163 25	−0.162 38
E_{lat}	−0.270 29	−0.325 65	−0.341 87	−0.347 80	−0.348 09	−0.347 64	−0.343 15	−0.336 30
Virial	−1.996 41	−1.998 41	−1.999 30	−1.999 83	−1.999 89	−2.000 28	−2.000 55	−2.000 73

IV. COHESIVE PROPERTIES OF THE NaF LATTICE

A. Equilibrium properties at zero pressure and temperature

We now present cohesive properties of the fcc NaF deduced from the PI results at several values of the sodium-fluoride distance R. In Table XII we collect E_{def}, $\frac{1}{2}E_{int}$, and E_{bind} for Na^+ and F^-, as well as the lattice energy and virial ratio obtained at eight values of R.

The positive deformation energies of Na^+ and F^- are decreasing functions of R, revealing an increasing reorganization of the electronic density at smaller distances. $E_{def}(Na^+)$ is very small even at 3.70 bohrs. Thus, according to Eq. (22), $E_{bind}(Na^+)$ is practically $\frac{1}{2}E_{int}(Na^+)$. The R dependence of the latter is very close to R^{-1}. The deformation energy of the F^- ion is much greater than $E_{def}(Na^+)$ (about 23 kcal/mol near R_e). The R dependence of $E_{int}(F^-)$ is very different from that of $E_{int}(Na^+)$ and shows a shallow minimum near R_e. $E_{bind}(F^-)$ is a decreasing function of R in the range analyzed here.

The lattice energy also shows a shallow minimum at $R_e = 4.481$ bohr, as can be observed in Fig. 6. Its curvature at R_e gives the bulk modulus

$$B = -V\frac{\partial P}{\partial V} = \frac{1}{18R_e}\left[\frac{\partial^2 U(R)}{\partial R^2}\right]_{R=R_e} . \tag{26}$$

The virial ratio plotted in Fig. 6 shows that the exact value is nearly satisfied at R_e. The agreement between our value for R_e and the observed one (4.378 bohrs, Table I) is most remarkable when we recall the results of elaborated multicenter cluster calculations. Winter, Pitzer, and Temple[6] found that the isolated $(NaF_6)^{5-}$ cluster has a continuously repulsive ground-state nuclear potential. The same result was found by Recio and Pueyo[51] using minimal Slater-type basis sets. When dressed with 26 point charges representing the nearer neighbors, this cluster shows a minimum at 5.38 bohrs.[6] If the sodium ions of these 26-member set are represented by total ion potentials, R_e becomes 4.54 bohrs.[6] The prediction improves further if the rest of the lattice is taken into account by simulating the Madelung potential.[6] The cluster-in-the-lattice calculation of Ref. 51, in terms of a pure electrostatic lattice, also gives a bound ground state.

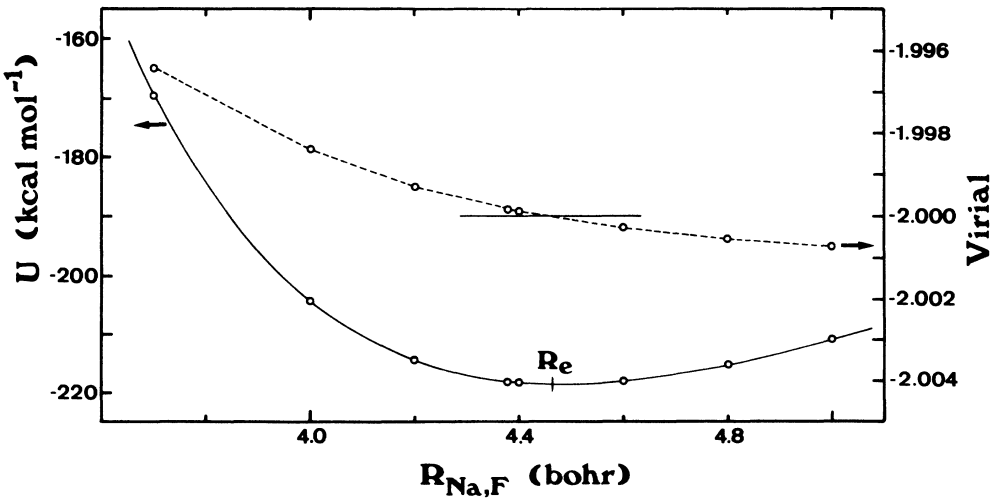

FIG. 6. Lattice energy (solid line) and virial ratio (dotted line) for NaF vs the internuclear distance.

TABLE XIII. Equilibrium properties of NaF at zero pressure and temperature.

Property	Expt.	PI value	Ref. 23
a (Å)	4.634[a]	4.742	4.88
ρ (g/cm^3)	2.803[a]	2.616	2.40
B (GPa)	46.5,[a] 51.4,[b] 51.7[c]	49.1	45.5
E_{lat} (kcal/mol)	−214.4,[a] −217.9,[d] −221[e]	−218.7	−211.9

[a]Reference 43.
[b]Data for 1 atm and 298 K, Ref. 53.
[c]Extrapolated value to 0 K, Ref. 54.
[d]Extrapolation to 0 K, Ref. 55.
[e]Reference 56, p. D-91.

As shown by Bermejo *et al.*,[52] the cluster-*in vacuo* level can give a very weakly bound ground state if a number of polarization functions are included in the calculation.

The significance of an adequate treatment of the cluster-lattice interaction in highly charged clusters like $(NaF_6)^{5-}$ is evident. By comparison with the model in Ref. 6, the PI scheme deals with a much more simple cluster but with a more detailed cluster-lattice interaction. In the language of the TES, the PI model represents a different lattice partition that emphasizes the cluster-lattice interaction by computing it in an *ab initio* way and maintaining cluster-lattice consistency.

The equilibrium properties of the NaF computed in this work at zero pressure and temperature are presented in Table XIII together with the observed values and the theoretical results obtained by Cohen and Gordon.[23] Since our PI calculation gives a value for R_e that is 0.11 Å larger than the experimental one, our computed density is 0.2 g/cm^3 smaller than the observed one (2.803 g/cm^3). We obtain 49.1 GPa for the bulk modulus. This value lies within the experimental range (46.5–51.7 GPa) reported by several authors.[43,53,54] The lattice energy computed at our theoretical geometry, −218.7 kcal/mol, differs by 0.3 kcal/mol from that obtained at the experimental geometry and agrees well with available experimental data that ranges from −214 to −221 kcal/mol.[43,55,56] Our results are comparable and even better than those from the semiempirical calculation in Ref. 23.

The variation of the NaF orbital energies with R is small: they change by less than 10% in the range $3.7 \le R \le 5.0$ bohrs (Fig. 7) and tend to their free-ion values when R increases. The ionic radial densities do not show any appreciable change with R in the range considered here. Even the deformation of the sensitivity $2p$ fluoride orbital is nearly independent of R.

B. Pressure effects on the equilibrium properties of the NaF

We will consider here the Gibbs free energy of the lattice:

$$G(R;P,T)=U(R)+PV(R)-TS(R)\ , \tag{27}$$

where U stands for lattice energy. At zero temperature,

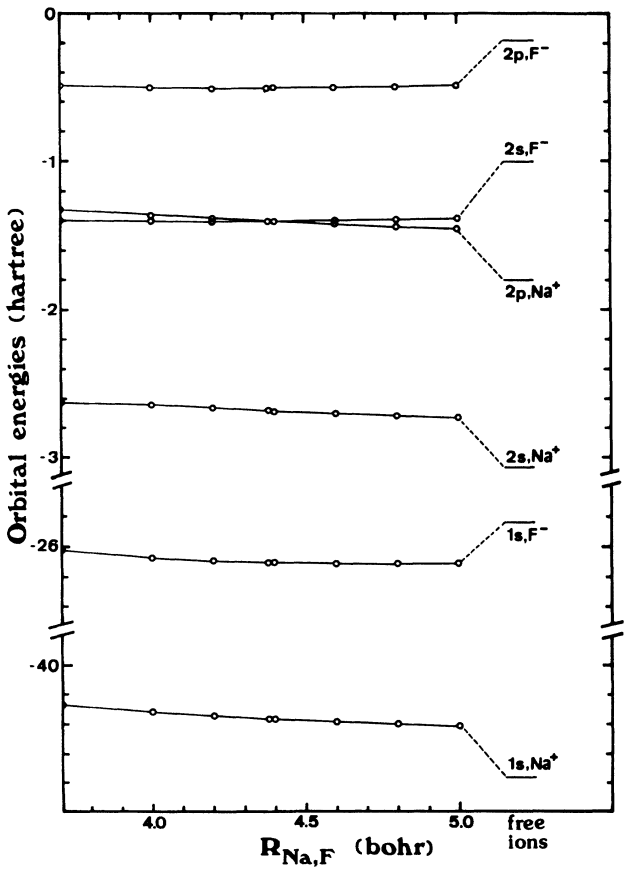

FIG. 7. PI orbital energies for NaF vs the internuclear distance.

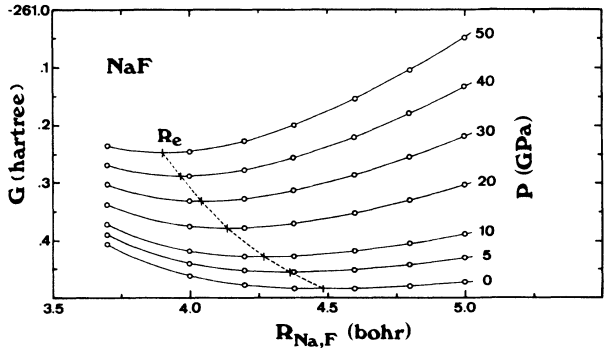

FIG. 8. Gibbs free-energy isobars for NaF as functions of the internuclear distance.

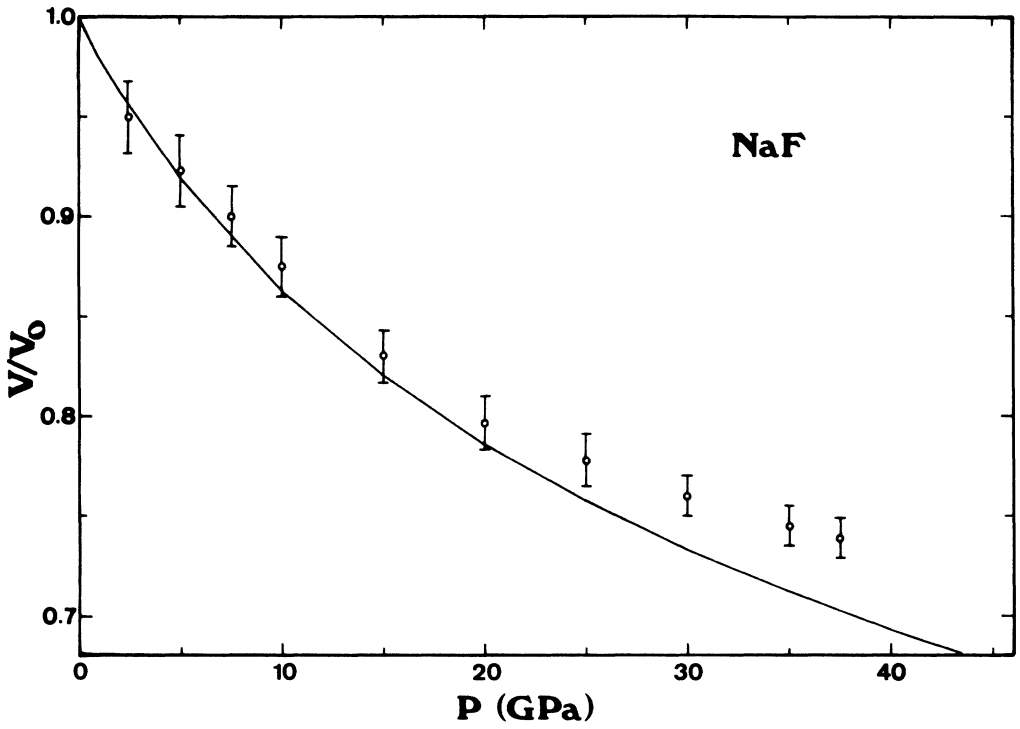

FIG. 9. PI values (solid line) for the relative cell volume of NaF vs the experimental data of Ref. 57.

we obtain $G(R;P,0)$ from $U(R)$, Fig. 6, and the molecular volume of the fcc phase $V=2R^3$. We will neglect any contribution from lattice vibrations.

In Fig. 8 we present seven $G(R;P,0)$ isobars for NaF, from $P=0$ to 50 GPa. Each isobar has a minimum at $R_e(P)$. The figure shows that $R_e(P)$ decreases with increasing pressure, in agreement with the observed results. Also, $G(R;P,0)$ increases with the applied pressure, as it should be. In Fig. 9 we plot the volume ratio V/V_0 versus the applied pressure. In this plot, V is $V(P=P, T=0)$, and V_0 is $V(P=0, T=0)$. Our theoretical curve can be compared with the room-temperature experimental data reported by Drickamer *et al.*[57] The PI results are compatible with these data up to 20 GPa.

The bulk modulus can be written as a function of P and T:

$$B(P,T)=\left|\frac{1}{18R}\frac{\partial^2 U}{\partial R^2}-\frac{1}{9R^2}\frac{\partial U}{\partial R}\right|_{R=R_e(P,T)}.$$

In Fig. 10 we present the pressure dependence of the theoretical $B(P,0)$ up to 45 GPa. This function is nearly linear within this range. Observed bulk moduli at zero pressure and temperature are available.[43,53,54] Also, the pressure dependence of B up to 1 GPa has been reported by Hart *et al.*[58,59] Thees data give B and its first and second pressure derivatives at zero pressure. Such values can be seen in Table XIV, together with our PI predictions. The theoretical zero-pressure B lies within the ex-

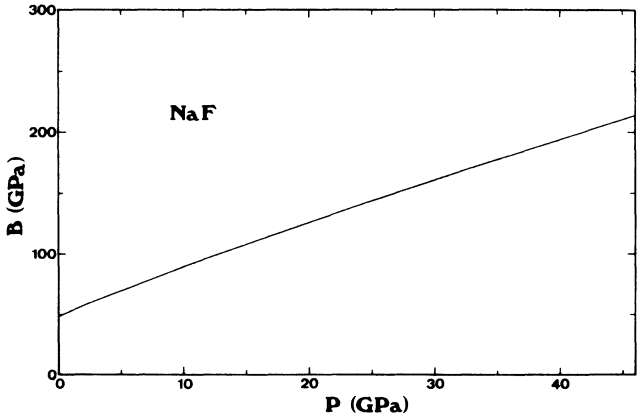

FIG. 10. Pressure dependence of the bulk modulus of NaF according to the PI calculation.

TABLE XIV. Bulk modulus and first and second pressure derivatives at zero pressure.

	Expt.	PI value
$B(P=0)$ (GPa)	46.5,[a] 51.4,[b] 51.7[c]	49.1
$dB/dP(P=0)$	5.03[d]	4.31
$d^2B/dP^2(P=0)$ (GPa^{-1})	−0.12[d]	−0.189

[a]Reference 43.
[b]Reference 53.
[c]Reference 54.
[d]Reference 58.

perimental range, and the PI values for the zero-pressure derivatives agree reasonably well with the observed data.

All these results are satisfactory and promising. They suggest that the PI method can be used to describe the equilibrium properties of more complex ionic crystals and, possibly, their variation with applied pressure.

V. CONCLUSIONS

We have developed a new theoretical scheme, the *ab initio* perturbed-ion method, adequate to analyze the electronic structure and chemical bonding of ionic crystal lattices. Following the theory of electronic separability, the *ab initio* model potential approach, and the restricted Hartree-Fock-Roothaan approximation, the PI method gives a set of atomic orbitals for each different lattice ion (the PI basis) that minimizes the ionic effective energy and ensures ion-lattice consistency. The PI basis is then used to compute the lattice energy and other properties of the crystal.

We have applied the PI method to nine alkali hydrides and halides and have found that the radial density of the cations remains almost unchanged in the process of crystal formation. The anionic radial density is contracted with respect to the free-ion curve: we find a charge transfer from the outer to the inner valence regions. The core regions remain unaffected. This change in the anionic electron density is mainly determined by the radial deformation of the outermost occupied orbital, it is almost independent of the interionic separation, and nearly the same for analogous crystals.

In the new method, the bonding mechanism is a combination of the orbital deformation just described and the ion-lattice quantum-mechanical interaction. In the binary systems considered, this mechanism raises the orbital energies of the cations and lowers those of the anions. Furthermore, the lattice energy of the crystal can be written as the sum of cationic and anionic binding contributions, each one containing a deformation and an interaction term. Our results show that although the anions show larger orbital deformation, the cations give larger contributions to the crystal binding.

Our computed lattice energies are in very good agreement with the thermochemical data for the fluorides. In other cases, they deviate as much as 30 kcal/mol. These deviations are assigned to lack of electron correlation and, to a minor extent, to insufficient variational freedom.

The orbital deformation upon crystal formation leads to detectable changes, with respect to the free-ion description, in those crystal properties mainly determined by outer operators. The diamagnetic susceptibility is an example of this type of observable. Properties determined by more internal operators, like the electronic form factors, remain essentially unaffected.

Finally, the PI method has been applied to analyze in more detail the cohesive properties of the NaF. In the limit of zero pressure and temperature, we find an equilibrium interionic distance 0.11 Å larger than the observed one and a bulk modulus within the experimental range. The crystal response to the applied pressure seems to be well described by the PI method up to 45 GPa.

It appears that the PI method, a TES-consistent cluster model in which the emphasis is centered on the cluster-lattice consistency and the quality of the cluster-lattice interaction more than on the size of the cluster, is able to give a reasonably accurate description of the bonding, stability, equilibrium properties, and pressure response of simple ionic crystals. We hope that the model could also be useful in the study of more complicated systems. We are presently exploring these applications and working on the elimination of the two main limitations of the present approach: the local-symmetry restriction on the active center and the closed-shell structure of the lattice ions. Removing of these two constraints should noticeably extend the domain of possible applications of the method.

ACKNOWLEDGMENTS

The authors are indebted to M. Bermejo and J. M. Recio for long and stimulating conversations; M. Bermejo also helped us with the figures. Financial support from the Dirección General de Investigación Científica y Técnica, (DGICyT) del Ministerio de Educación y Ciencia (Spain) under Project No. PB86-0240, is gratefully acknowledged.

*Present address: Department of Chemistry, Ohio State University, Columbus, OH 43210.

[1]S. Sugano and R. G. Shulman, Phys. Rev. **130**, 517 (1963).
[2]R. Dovesi, C. Ermodi, E. Ferrero, C. Pisani, and C. Roetti, Phys. Rev. B **29**, 3591 (1984).
[3]N. E. Brener and J. Callaway, Phys. Rev. B **35**, 4001 (1987).
[4]G. J. M. Janssen and W. C. Nieuwpoort, Phys. Rev. B **38**, 3449 (1988).
[5]S. Y. Shashkin and W. A. Goddard III, Phys. Rev. B **33**, 1353 (1986).
[6]N. W. Winter, R. M. Pitzer, and D. Temple, J. Chem. Phys. **86**, 3549 (1987).
[7]N. W. Winter, R. M. Pitzer, and D. Temple, J. Chem. Phys. **87**, 2945 (1987).
[8]N. W. Winter and R. M. Pitzer, J. Chem. Phys. **89**, 446 (1988).
[9]A. B. Kunz and J. M. Vail, Phys. Rev. **38**, 1058 (1988).
[10]A. B. Kunz, J. Meng, and J. M. Vail, Phys. Rev. **38**, 1064 (1988).
[11]Z. Barandiarán and L. Seijo, J. Chem. Phys. **89**, 5739 (1988).
[12]Z. Barandiarán and L. Pueyo, J. Chem. Phys. **79**, 1926 (1983).
[13]S. Huzinaga, L. Seijo, Z. Barandiarán, and M. Klobukowski, J. Chem. Phys. **86**, 2132 (1987).
[14]A. B. Kunz and D. L. Klein, Phys. Rev. B **17**, 4614 (1978).
[15]V. Luaña, Ph.D. thesis, Universidad de Oviedo, 1987.
[16]V. Luaña, E. Franciso, M. Flórez, J. M. Recio, and L. Pueyo, J. Chim. Phys. **84**, 863 (1987).
[17]V. Luaña and L. Pueyo, Phys. Rev. B **39**, 11 093 (1989).
[18]V. Luaña, M. Bermejo, M. Flórez, J. M. Recio, and L. Pueyo, J. Chem. Phys. **90**, 6409 (1989).
[19]S. Huzinaga and A. A. Cantu, J. Chem. Phys. **55**, 5543 (1971).

[20]S. Huzinaga, D. McWilliams, and A. A. Cantu, Adv. Quantum Chem. **7**, 187 (1973).
[21]V. Luaña and L. Pueyo, J. Mol. Struct. (Theochem) **15**, 45 (1988).
[22]Y. S. Kim and R. G. Gordon, Phys. Rev. B **9**, 3548 (1974).
[23]A. J. Cohen and R. G. Gordon, Phys. Rev. B **12**, 3228 (1975).
[24]J. Yamashita and M. Kojima, J. Phys. Soc. Jpn. **7**, 261 (1952).
[25]T. Hoshino, T. Asada, and K. Terakura, Phys. Rev. B **31**, 2005 (1985).
[26]S. Katsuki, Chem. Phys. Lett. **127**, 231 (1986).
[27]R. K. Jeck and J. J. Krebs, Phys. Rev. B **5**, 1677 (1972).
[28]A. L. Wachs, P. E. A. Turchi, Y. C. Jean, K. H. Wetzler, R. H. Howell, M. J. Fluss, D. R. Harshman, J. P. Remeika, A. S. Cooper, and R. M. Fleming, Phys. Rev. B **38**, 913 (1988).
[29]A. B. Kunz, Phys. Rev. B **26**, 2056 (1982).
[30]J. Yamashita and S. Asano, J. Phys. Soc. Jpn. **52**, 3506 (1983).
[31]J. Yamashita and S. Asano, J. Phys. Soc. Jpn. **53**, 3112 (1984).
[32]W. P. Menzel, K. Mednick, C. C. Lin, and C. F. Dorman, J. Chem. Phys. **63**, 4708 (1975).
[33]M. J. Mehl, R. J. Hemley, and L. L. Boyer, Phys. Rev. B **33**, 8685 (1986).
[34]R. McWeeny and B. T. Sutcliffe, *Methods of Molecular Quantum Mechanics* (Academic, London, 1969).
[35]P. G. Lykos and R. G. Parr, J. Chem. Phys. **24**, 1166 (1956).
[36]R. G. Parr, R. O. Ellison, and P. G. Lykos, J. Chem. Phys. **24**, 1106 (1956).
[37]G. Höjer and J. Chung, Int. J. Quantum Chem. **14**, 623 (1978).
[38]V. Luaña and L. Pueyo, Int. J. Quantum Chem. **31**, 975 (1987).
[39]V. Bonifacic and S. Huzinaga, J. Chem. Phys. **60**, 2779 (1974); **62**, 1507 (1975); **62**, 1509 (1975); **64**, 956 (1976); **65**, 2322 (1976).
[40]C. C. J. Roothaan and P. S. Bagus, in *Methods in Computational Physics,* edited by B. Alder, S. Fernbach, and M. Rotenberg (Academic, New York, 1963), Vol. 2, p. 47.
[41]V. Luaña and L. Pueyo (unpublished).
[42]P. P. Ewald, Ann. Physik (Leipzig) [Folger 4] **64**, 253 (1921).
[43]M. P. Tosi, in *Solid State Physics,* edited by H. Ehrenreich, F. Seitz, and D. Turnbull (Academic, New York, 1964), Vol. 16, p. 1.
[44]A. G. Piken and W. Van Gool, Ford Motor Company Technical Report No. S168-10, 1968 (unpublished).
[45]W. Van Gool and A. G. Piken, J. Mater. Sci. **4**, 95 (1969).
[46]E. Clementi and C. Roetti, At. Data Nucl. Data Tables **14**, 177 (1974).
[47]It is necessary to recall that the approach of Gordon and coworkers (Refs. 23 and 24) differs from the PI calculation in several important points. Their method is not variational and includes an approximate representation of the electron correlation. Also, the (free-ion) electron density is a datum rather than a result of their analysis. The PI approach is a variational calculation of the ionic electron density in the crystal and does not include (in the present version) electron correlation.
[48]J. H. Van Vleck, *The Theory of Electric and Magnetic Susceptibilities* (Oxford University Press, London, 1966).
[49]J. C. Davis, Jr., *Advanced Physical Chemistry* (Roland, New York, 1965).
[50]S. Fraga, J. Karwowski, and K. M. S. Saxena, *Handbook of Atomic Data* (Elsevier, Amsterdam, 1976).
[51]J. M. Recio and L. Pueyo, J. Mol. Struct. (Theochem) **166**, 209 (1988).
[52]M. Bermejo, V. Luaña, J. M. Recio, and L. Pueyo, J. Mol. Struct. (Theochem) **166**, 235 (1988).
[53]J. T. Lewis, A. Lehoczky, and C. V. Briscoe, Phys. Rev. **161**, 877 (1967).
[54]J. Vallin, K. Marklund, J. O. Sikström, and O. Beckman, Ark. Fys. **32**, 515 (1966).
[55]Extrapolated value to 0 K, by L. Brewer, in C. Kittel, *Introduction to Solid State Physics,* 4th ed. (Wiley, New York, 1971), p. 121.
[56]*Handbook of Chemistry and Physics,* edited by R. C. Weast, 60th ed. (Chemical Rubber Co., Boca Raton, FL, 1979).
[57]H. G. Drickamer, R. W. Lynch, R. L. Clendenen, and E. A. Pérez-Albuerne, in *Solid State Physics,* edited by H. Ehrenreich, F. Seitz, and D. Turnbull (Academic, New York, 1965), Vol. 19, p. 135.
[58]S. Hart and P. H. Greenwood, Solid State Commun. **46**, 161 (1983).
[59]S. Hart, Mater. Res. Soc. Symp. Proc. **22**, 239 (1984).
[60]F. A. Cotton and G. Wilkinson, *Advanced Inorganic Chemistry,* 2nd ed. (Wiley, New York, 1966).
[61]C. R. Fischer, T. A. Dellin, S. W. Harrison, R. D. Hatcher, and W. D. Wilson, Phys. Rev. B **1**, 876 (1970).
[62]T. C. Waddington, Adv. Inorg. Chem. Radiochem. **1**, 157 (1959).
[63]H. J. F. Jansen and A. J. Freeman, Phys. Rev. B **33**, 8629 (1986).
[64]C. E. Moore, National Bureau Standards Report No. NSRDS-NBS34, Washington, D.C., 1979.